Sports Eng (2011) 13:95–104
DOI 10.1007/s12283-010-0054-z

ORIGINAL ARTICLE

Bowling ball dynamics revealed by miniature wireless MEMS inertial measurement unit

Kevin King · N. C. Perkins · Hugh Churchill · Ryan McGinnis · Ryan Doss · Ron Hickland

Published online: 1 October 2010

Abstract This paper presents a novel sensor technology to deduce the dynamics of a bowling ball. The sensor, a miniature wireless inertial measurement unit (IMU), incorporates MEMS accelerometers and angular rate gyros, a microcontroller, a low power RF transceiver, and a rechargeable battery. When embedded in a bowling ball, the IMU transmits the acceleration and angular velocity data that define the dynamics of the ball starting with the bowler's delivery and its motion in the lane. Example results from professional bowlers illustrate how this technology can be used to assess bowler skill and ball performance. For instance, the IMU accurately measures the spin dynamics of the ball which are crucial to develop the ball "hook." An analysis of ball dynamics in the lane is distilled to a measurable "hook potential" metric for further assessing bowler skill. Finally, the sensor presented herein is believed to be the world's smallest, wireless IMU. This highly miniaturized and wireless design will enable parallel training systems for many sports, including basketball, baseball, crew, cricket, golf, fly fishing, soccer, softball, tennis, rowing, among others.

Keywords Tenpin bowling · Sports training · Dynamics · Inertial Sensors

K. King · N. C. Perkins (✉) · H. Churchill · R. McGinnis · R. Doss
Mechanical Engineering, University of Michigan, 2350 Hayward Street, Ann Arbor, MI 48109-2125, USA
e-mail: ncp@umich.edu

R. Hickland
Ebonite International, Hopkinsville, KY 42240, USA

1 Introduction

The sport of tenpin bowling is popular worldwide and accessible to many. In the US alone, more than 66 million people bowl every year and over 2 million of these compete regularly in league play certified by the United States Bowling Congress (USBC) [1]. Worldwide, and in over 90 countries, more than 100 million bowlers play the sport, a rate of participation second perhaps to only football/soccer. Of course, as with any sport, success in bowling requires directed practice to develop specific skills.

A major skill in bowling is the ability to release the ball on the lane so that the subsequent ball path curves or "hooks" near the end of the lane prior to impact with the pins. The hook allows the ball to enter the "pocket" in the pins (between the first or "head" pin and the second row of pins) in a direction that maximizes the chances for a "strike". The hook, created by the sideways component of ball/lane friction, derives from ball spin. In particular, the component of angular velocity vector parallel to the trajectory of the ball, known as "side spin" (analogous to "rifle spin") contributes greatly to the sideways friction force. The ability to consistently generate large and controllable side spin is a hallmark of an expert bowler. All other factors that influence the friction on the ball also influence the hook including the pattern of oil on a prepared lane, the lane material, the lubrication properties of the outer layer or "coverstock" of the ball, and the precessional motion of the ball that brings "fresh" (un-oiled) ball surfaces into contact with the lane.

The dynamics of a bowling ball on a lane, or more generally a sphere in frictional contact with a surface, is a fascinating problem in rigid body dynamics that has also received considerable attention in the literature [2–11] including treatments as examples in mechanics textbooks

[2, 3]. A focused treatment of the hook shot in bowling is provided by Hopkins and Patterson [4], who demonstrate that the path of the ball center is parabolic under the assumptions of a radially symmetric ball and spatially uniform ball/lane friction. In this instance, the Newton–Euler equations governing the five degrees of freedom of the ball on the lane can be solved in closed form (per [2, 3]) and they reveal that the friction force remains constant (both magnitude and direction) if the ball is rolling with sliding. If/when the ball transitions to rolling without sliding, the ball path becomes linear (and bowlers often say that the ball has "run out"). Huston et al. [5] relax assumptions in [2–4] by considering balls whose non-radially symmetric cores create (1) an offset of the mass center from the geometric center and/or (2) non-degenerate (i.e. distinct) principal moments of inertia (to foster ball precession). In addition, they allow the ball/lane friction to vary with position in the lane. For describing ball orientation, Huston et al. [5] employs Euler parameters which then avoid the singularities associated with the Euler angles later employed by Frohlich [6] in what is otherwise an identical model. Taken together, the two studies [5, 6] present numerical solutions to the Newton–Euler equations that illustrate how the hook can depend on the initial conditions of the ball at release, the mass distribution of the ball, and the (potentially non-uniform) friction properties along the lane. In particular, the initial or "release" conditions influencing the hook include: (1) the magnitude of the angular velocity at release (what bowlers refer to as the "rev rate"), (2) the direction of the angular velocity at release (what bowlers refer to as the "axis point"), and (3) the speed of the ball center. The mass distribution properties that may also influence the hook include: (1) the mass center offset and (2) the unequal principal moments of inertia arising from a non-radially symmetric core. Similarly, Zecchini and Foutch [7] consider both radially and non-radially symmetric balls (yet with no mass center offset) and in so-doing largely confirm prior results [4, 5] while also illustrating favorable comparisons to experimental measurements of the ball path. While revisiting the analysis of radially symmetric balls, Walker [8] concludes that the angle at which the ball strikes the pins in the pocket (what bowlers refer to as the "entry angle") depends solely on the side spin and speed of the ball center at release, and not on the lane friction. Under the assumptions employed in Walker [8], the lane friction dictates where the transition from rolling with sliding to rolling without sliding occurs (and hence the total displacement of the ball across the lane), but not the entry angle. Like all of the studies above, this study clearly demonstrates the enormous influence of the ball release conditions in creating the hook.

Related to tenpin bowling is the sport of lawn bowling which employs non-spherical balls that largely roll without sliding on prepared lawn surfaces. Specific to this case (rolling without sliding), Cross [9] develops an analytical solution for the ball path from which he demonstrates that the path curvature derives from precession. In this context, dissipation derives from the rolling resistance of the ball on a deformable (grass) medium which is decidedly different from the sliding friction acting on a bowling ball. The interested reader may also wish to refer to prior analyses of lawn bowls [10, 11].

Relative to the theoretical studies above, fewer studies contribute experimental measurements of the dynamics of a bowling ball, particularly during the delivery and release. Existing lane ball monitors currently track ball position and speed in the lane, but not while the ball is being thrown. Chu et al. [12] present a video motion capture study of bowler delivery by resolving the ball path and that of critical body landmarks (e.g. feet, hip, shoulder and wrist) in the sagittal plane. Noted differences between female and male bowlers are emphasized. The forces and moments imparted to the ball by the bowler's hand are reported by Fuss [13] using a ball instrumented with three (6-axis) load cells. After cutting the ball in half and removing sections, three load cells are installed around the thumb and finger hole recesses. The re-assembled ball, which incorporates a wiring harness to external signal conditioners and a power supply, is thrown to a bed of foam a short distance away. The force and moment histories for three types of shots (straight, hook, and spin) reveal that better bowlers apply larger forces and moments to the ball, impart larger pinch forces, and develop larger and longer impulses during the forward swing.

Clearly, the dynamics of a bowling ball down the lane is determined by the instantaneous velocity and angular velocity of the ball when it is released from the bowler's hand (as well as all other factors influencing ball friction). Knowing these, "initial" or "release" conditions is vital to understanding both player skill and ball design. Fortunately, precise measurements of these (and many other) characteristics of ball motion are now possible through the advent of miniature microelectromechanical system (MEMS) inertial sensors; see, for example [14–16]. Common MEMS inertial sensors include tri-axis accelerometers which detect the acceleration of a point and single-, dual- and now tri-axis angular rate gyros which detect the components of the angular velocity of the body to which they are attached. When combined to form a complete strap-down inertial measurement unit (IMU) [17–19], these inertial sensors detect the six degrees of freedom of a rigid body in space by sensing the acceleration (vector) of one point on the body as well as the angular velocity (vector) of the body. When mounted on or within sports equipment, a miniature IMU provides the essential data needed to resolve the motion of that equipment as disclosed by

Perkins [20, 21]. Novel MEMS-based sports training systems have been developed for golf [22–25] and for fly fishing [26, 27], among additional applications currently underway. Other examples include [28, 29].

As applied to the sport of bowling, Hon et al. [30] employ a commercial wireless IMU mounted to the bowler's forearm to measure forearm motion. An overview of the hardware and software are presented as are the results from one trial. Unfortunately, strapping the sensor to the bowler's forearm renders this approach invasive (and potentially uncomfortable) and it also eliminates the ability to measure the actual dynamics of the bowling ball due to significant dynamics contributed by the (unmonitored) wrist and finger joints. The interested reader should also be aware of an erroneous interpretation made in Hon et al. [30] of the forearm angular velocity depicted in Fig. 6, which is discussed in the results section of this paper.

This paper presents a highly miniaturized wireless IMU (also believed to be the world's smallest) that can be readily embedded within an actual bowling ball. Our technology, therefore, yields the means to directly measure the dynamics of the ball during both the delivery phase and its subsequent motion down the lane. We open in Sect. 2 by describing the new, highly miniaturized wireless IMU. In Sect. 3, we highlight the capabilities of this design for the sport of bowling by carefully examining the angular velocity, linear velocity, and orientation of the ball for example shots made by professional bowlers. Section 4 contributes an analysis of the friction force acting on a bowling ball and distills this analysis to a measurable "hook potential" metric for further assessing bowler skill. We close with our summary and conclusions in Sect. 5.

2 Miniature wireless IMU for bowling ball dynamics

2.1 IMU design and installation in a bowling ball

The measurements described in this paper are obtained using the highly miniaturized wireless IMU illustrated in Fig. 1 that was developed for sports training and general human motion applications. This single-board design, which is believed to be the world's smallest wireless IMU, follows a lineage of larger, multi-board IMU designs developed in our laboratory [22–25].

The two faces of the design separate analog and digital circuits. The MEMS inertial sensors mounted on the analog circuit side (Fig. 1a), include a three-axis accelerometer, one dual-axis and one single-axis angular rate gyros, op-amps for signal integrity, and off-chip components for filtering. The digital circuit side (Fig. 1b) includes a microprocessor for AD conversion, a low power RF transceiver, and a small surface mount antenna; also, visible are

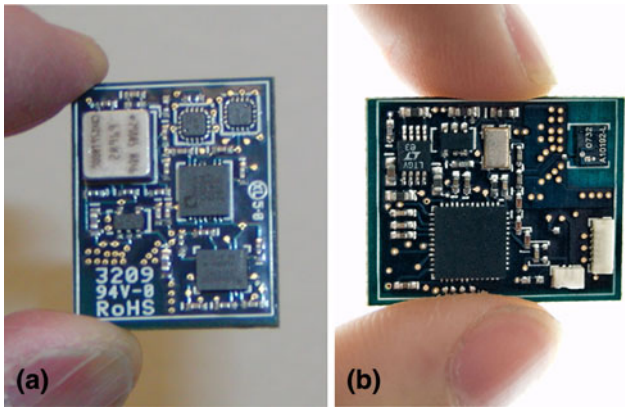

Fig. 1 Highly miniaturized wireless IMU. **a** Analog circuit side with MEMS angular rate gyros and accelerometer, **b** digital circuit side with microprocessor, wireless transceiver, surface mount antenna, and connectors for battery power and firmware programming

two small connectors (white, lower right) that provide battery connection and the (one-time) connection to a host computer for downloading microprocessor firmware.

The minimized footprint (19 × 24 mm) is achieved using a six-layer board containing four internal planes: two for interconnects and one each for power and ground. The assembled IMU board has a mass of 3.0 g and the associated miniature lithium-ion battery adds a mere 1.5 g. The power draw remains below 25 mW and the battery tank yields 4 h of uninterrupted use between recharging. The microprocessor performs 12-bit A/D conversion and, for the application herein, provides 1 kHz sampling of all sensor channels. The low-power RF transceiver uses a proprietary RF protocol to transmit over a typical open-air range of 15–60 feet (4.57–18.29 m) with 60 feet (18.29 m) being achieved in very low ambient RF environments (as in bowling centers). This is a commercial 2.45 GHz RF transceiver (Nordic^{TM}) that has a packet latency of 1 ms. A USB-enabled receiver (not shown) allows data collection on a host (laptop) computer via custom data collection software. Before first use, the IMU is calibrated following a procedure described in King [22]. Doing so provides a system level calibration matrix that yields the sensitivities and cross-axis sensitivities of the three accelerometer axes and the three angular rate gyro axes.

The IMU and a rechargeable (lithium-ion) battery are shrink wrapped to form a small sensor module for insertion into a bowling ball as shown in Fig. 2. The module is first inserted into a modified "thumb slug." Thumb slugs, which are often used by experienced bowlers, are captured in a thumb hole via a sleeve which locks the slug in place. For our study, a separate hole is drilled into the ball at a convenient, but known location relative to the center of the grip (it would also be possible to embed the tiny sensor

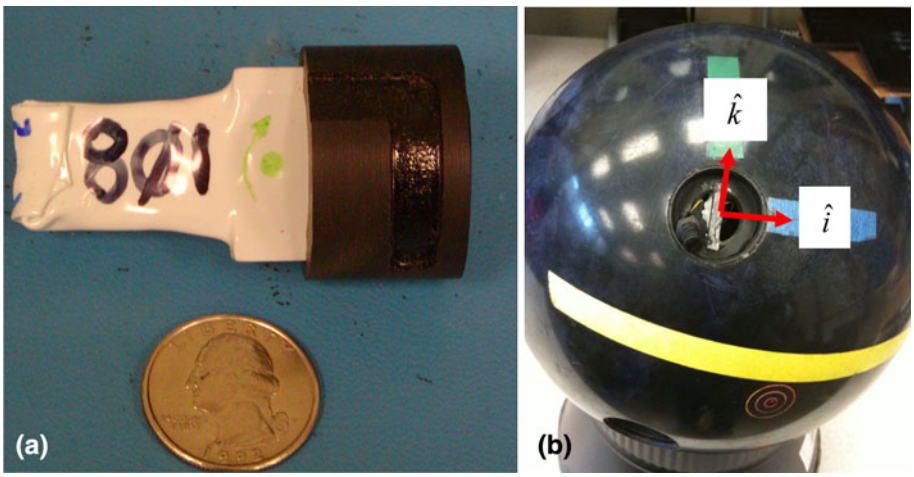

Fig. 2 **a** Shrink-wrapped IMU and battery (*white*) installed in a modified thumb slug (*black*). **b** Thumb slug installed in a bowling ball via standard *thumb insert*. The illustrated frame $(\hat{i},\hat{j},\hat{k})$ denotes the sense axes of the inertial sensors (accelerometers and angular rate gyros)

within the actual thumb hole). The net result is that the sensor is held securely in this new hole with the antenna near the surface of the ball to maximize signal transmission. Moreover, the position and orientation of the accelerometer are known relative to important features of the ball including the ball center and the grip center.

2.2 Data collection and experimental procedure

Included in this design is a small recharging plug and jack which enables recharging via a USB cable connection to a host computer. When the recharging plug is removed, the sensor is powered by the internal battery and continuously transmits data to the host computer. When the plug is reinserted, the battery power is switched off and transmission ceases (and the battery can also be recharged if needed).

A trial is performed by first holding the ball stationary momentarily and then executing a "throw" (or "shot") in an otherwise unencumbered manner. Data collection continues for a prescribed period of time (typically 15 s) as determined by custom data collection software. Following a throw, the IMU data can be promptly analyzed to yield results as described next.

3 Assessing bowler skill and ball performance

Consider first data obtained from the embedded angular rate gyros that measure the angular velocity of the ball. Figure 3 illustrates the magnitude of the angular velocity, what bowlers refer to as the "rev rate" in the units of revolutions per minute (RPM), as a function of time for an example trial by a professional bowler. The rev rate is obtained by taking the magnitude of the vector sum of the three angular rate gyro signals and then reporting the magnitude in the units of RPM. Clearly distinguishable in this figure are the major phases of ball motion that include the initial period of time the ball is held at rest ($0 < t < 1.5$ s), followed by the throw made by the bowler ($1.5 < t < 3.9$ s), and then the period of time the ball slides/rolls on the lane ($3.9 < t < 6.1$ s). The bowler's throw initiates ball rotation and this concludes just prior to when the ball impacts the lane producing a discernible spike in the data ($t = 3.9$ s). A second impact (second discernable spike) occurs the instant the ball first strikes a pin near the end of the trial ($t = 6.1$ s). As is typical of professional bowlers, this bowler generates considerable rev rate (305 RPM or 31.9 rad/s) at the very end of the throw as described in detail below. The ball rev rate continues to increase as the ball rolls down the lane, and this increase is substantial just prior to pin impact. As also described below, the angular velocity of the ball increases as the ball transitions from rolling with sliding to rolling without sliding in the last (oil-free) section of the lane.

The major phases of the throw were independently confirmed using high-speed video photography and with a frame rate of 300 frames per second. The high-speed video was synchronized with the IMU data using the ball impact on the lane as the synchronization event. A custom-written Matlab^{TM} code enables us to produce a new video that simultaneously displays the video images of the ball with the time-history of the ball rev rate; see example posted at http://wwwpersonal.umich.edu/~ryanmcg/BowlingProject.html

In Fig. 3, the bowler's throw is further decomposed into the back swing (gray), the forward swing or "delivery" (red) and the release (green). During the back swing ($1.5 < t < 3.2$ s) the bowler's arm swings opposite the direction of the pins. At the end of the back swing, the ball achieves its maximum height and, simultaneously, the angular velocity of the ball approaches zero. The interested reader should also be aware of an erroneous interpretation made in Hon et al. [30] of the forearm angular velocity

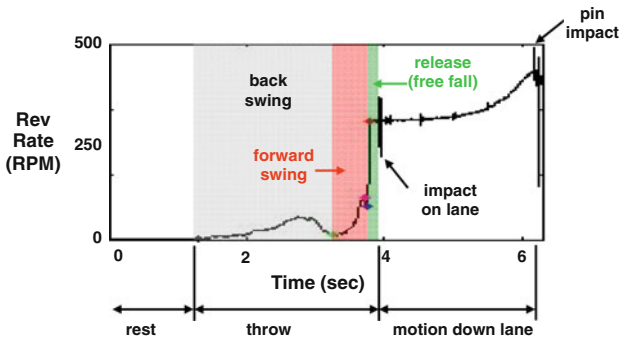

Fig. 3 The major phases of ball motion as revealed by the ball rev rate (magnitude of angular velocity). Rev rate (RPM) as a function of time during the rest phase, the bowler's "throw", and the motion down the lane

depicted in Fig. 6. The maximum height in the back swing occurs when the forearm angular velocity passes through zero and not when it achieves a maximum value as claimed therein. During the forward swing ($3.2 < t < 3.8$ s), the bowler's arm swings rapidly towards the pins. The ball rev rate now increases and dramatically so at the very end of the forward swing, just prior to ball release. Immediately thereafter, the ball is in free fall for a very short period of time before it impacts the lane. The ability to generate a large rev rate is a skill of expert bowlers. How this large rev rate arises is clearly revealed in the exploded view of the bowler's "throw" illustrated in Fig. 4.

The top portion of Fig. 4 illustrates the rev rate (magnitude of angular velocity) during the back swing (gray area), the forward swing (red area), the release and the subsequent free fall of the ball (green area). Note that at the end of the back swing, the ball has near-zero rev rate as expected. The ball and the bowler's arm then execute a pendulum motion as the bowler continues walking towards the foul line. During this pendulum motion, the angular velocity of the ball describes ball motion in the (vertical) plane of the forward swing which builds ball speed prior to release. Moreover, the bowler's palm is largely under and behind the ball during this phase. Just prior to release, however, the bowler tends to rotate his palm inwards while releasing his thumb from the thumb hole. In this new position (palm more on the outside of the ball), the bowler immediately pulls upwards with the two fingers still embedded in the finger holes. This lifting action, referred to by bowlers simply as the "lift", generates a substantial moment on the ball and a dramatic increase in the rev rate (i.e. a dramatic angular acceleration). Moreover, a large component of this moment is directed about a horizontal axis (pointing back towards the bowler for a right-handed bowler or pointing towards the pins for a left-handed bowler). The angular acceleration and hence the resulting large angular velocity prior to release is, therefore, directed about this horizontal spin axis and leads to the "side spin"

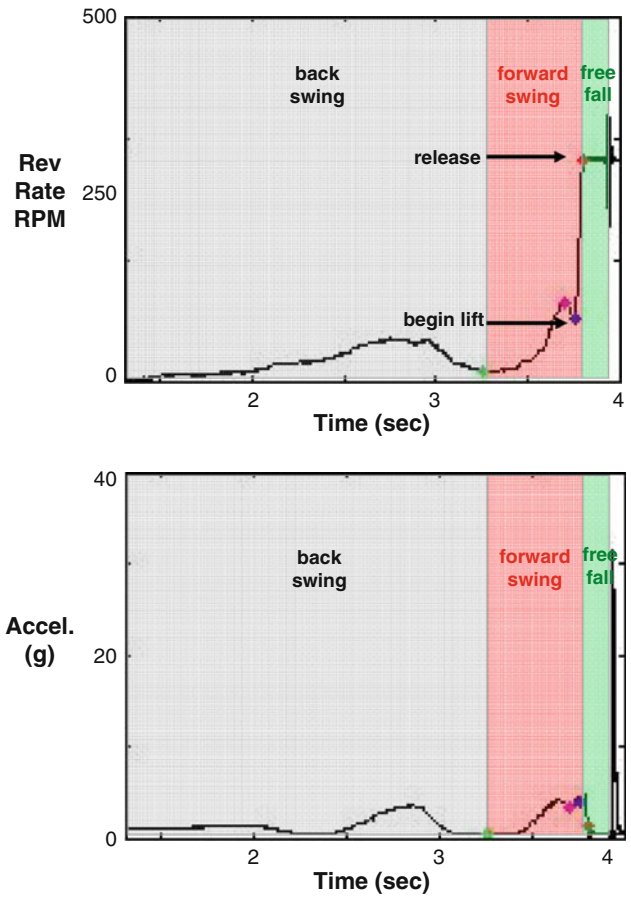

Fig. 4 Exploded view of the "throw" phase for a professional bowler that includes the back swing, the forward swing, and the release and subsequent free flight of the ball. *Top figure* illustrates the ball rev rate (magnitude of angular velocity). Note the large increase in rev rate from the beginning of the lift to release. *Bottom figure* illustrates the associated acceleration magnitude of the ball center

(or "rifle spin") required for the ball to hook in the lane. Note carefully that the lift, which is so visible in Fig. 4, develops in a mere 50 ms, but yields more than a threefold increase in the rev rate (from 85 to 305 RPM or 8.9 to 31.9 rad/s) in this typical example for a professional bowler. Next, the instant the hand releases from the ball is readily detectable since, at this instant, the angular acceleration suddenly vanishes. During the subsequent free flight phase (green area), there is no measurable (drag-induced) moment applied about the mass center of the ball and therefore the angular momentum of the ball about the mass center remains conserved for this short (but readily detectable) time interval. The associated acceleration (magnitude) of the center of the ball is reported in the lower portion of Fig. 4 (in the units of g's). At the conclusion of the forward swing at release, there is a dramatic decrease in the acceleration. This is expected since, during free flight, the acceleration of the ball center reduces to 1 g.

The dynamics of the ball down the lane are dictated by the linear and angular velocity of the ball at release (as well as by all factors influencing ball/lane friction). As illustrated above, the embedded IMU directly measures the angular velocity $\vec{\omega}$, and the value of this vector at release is also readily detectable. In addition, the IMU directly measures the acceleration of one point in the ball (the location of tri-axis accelerometer). Using the measured angular velocity and acceleration, one can then compute the velocity of the ball center following established kinematical algorithms. For example, the measurement theory of [22, 23] details how one can obtain the velocity of any point on a rigid body by appropriate integration of the angular velocity and acceleration data obtained from an embedded IMU. In lieu of duplicating this published procedure, we outline next the major steps.

The MEMS accelerometer measures the acceleration of the point "a" on the ball coincident with the location of the accelerometer. Moreover this acceleration vector, which is defined with respect to the ball-fixed frame of reference $(\hat{i},\hat{j},\hat{k})$ illustrated in Fig. 2, also includes the superimposed acceleration due to gravity $\vec{g}$. This acceleration vector must first be resolved into components lying within and perpendicular to the plane of the lane, that is, a "lane-fixed" frame. This is accomplished by computing the direction cosine matrix relating the ball-fixed and lane-fixed frames. The direction cosine matrix follows from integrating the angular velocity vector. Once transformed to the lane-fixed frame, the acceleration due to gravity can now be subtracted, and the resulting acceleration components can be integrated in time to yield the velocity vector $\vec{v}_a$ of the point "a" coincident with the accelerometer and in the lane-fixed frame of reference. The velocity of the ball center than follows using the elementary relationship $\vec{v} = \vec{v}_a + \vec{\omega} \times \vec{r}$ where $\vec{\omega}$ is the measured angular velocity of the ball (via angular rate gyros) and $\vec{r}$ is the a priori measured position of the ball center relative to point a. The latter term must also be transformed to the lane-fixed frame via the direction cosine matrix described above. The calculation sequence is identical to that previously described in detail in King et al. [23]. The speed of the ball center calculated from the IMU data was also benchmarked against that obtained using a standard radar gun which reports speeds to a resolution of 0.1 mph (0.045 m/s). Over 30 trials, the average difference between the calculated speed and the speed reported by the radar gun is 2.9%.

Figure 5 illustrates the "release conditions" $(\vec{\omega},\vec{v})$ for an example throw by a right-handed professional bowler. Also shown are the thumb and finger holes and the position of the center of the grip (denoted by C). Notice that the angular velocity vector is directed nearly opposite the ball

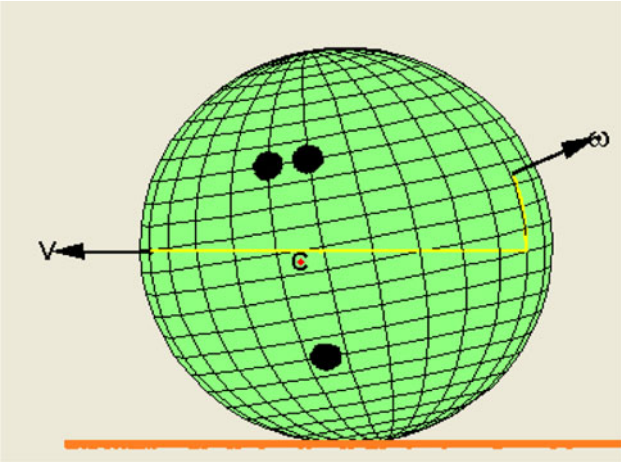

Fig. 5 The angular velocity $\vec{\omega}$ and velocity of the ball center $\vec{v}$ at release for a right-handed professional bowler. The center of the grip is denoted by C

center velocity. In other words, $\vec{\omega}$ largely points back at the bowler confirming the large "side roll" imparted to the ball during the lift. The spin axis at release defines the so-called bowler's "axis point"; namely, the point where $\vec{\omega}$ pierces the ball surface. In the illustrated example, this initial axis point lies $x = 5.56$ in. (14.1 cm) to the right and $y = 1$ in. (2.5 cm) above the center grip C, where the (x, y) surface coordinates form the orthogonal grid superimposed on the ball [in this grid, 1 unit along x and 1 unit along y corresponds to 1 in. (2.5 cm) and 0.5 in. (1.3 cm), respectively]. The position of the initial axis point relative to the velocity $\vec{v}$ greatly influences the potential of the ball to hook as given in the analysis that follows.

Following the release, the ball impacts the lane and initially rolls with sliding on the oiled lane surface. The friction force of the lane on the ball imparts a net moment about the ball mass center and this moment changes both the magnitude and the direction of the angular momentum hence $\vec{\omega}$. Thus, the instantaneous axis point migrates on the surface of the ball as illustrated in Fig. 6a. In this example, the initial axis point is denoted by point A, and the instantaneous axis point (spin axis) migrates in the direction of the thumb hole along the red curve. This axis migration is not only a function of the friction force; it is also a strong function of the inertia tensor of the bowling ball. In particular, bowling balls are often intentionally designed to have distinct principal moments of inertia and the axis migration scales with the difference between the major and minor moments of inertia when the ball is thrown properly. The simulations [5–7] specifically account for the inertia properties of non-radially symmetric balls and thus capture the resulting precession of the spin axis. If the axis point did not migrate, then the spin axis

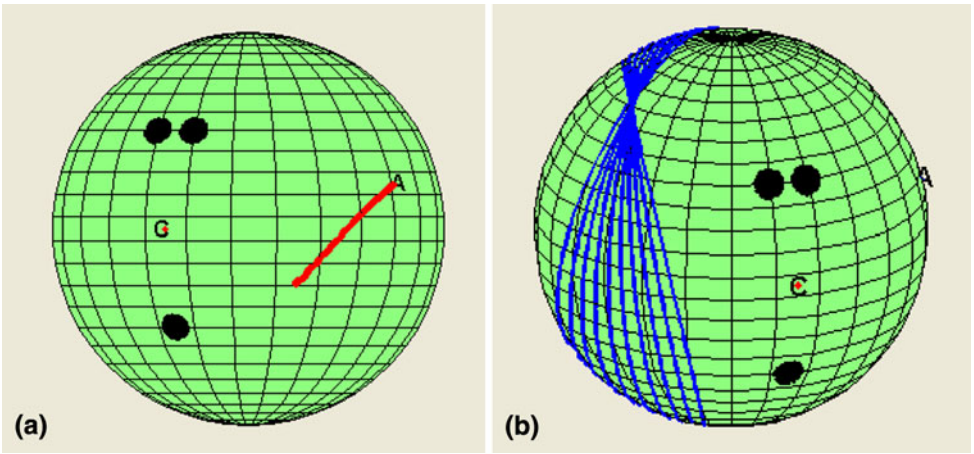

Fig. 6 **a** The initial axis point (at release) is designated by point *A* and migrates towards the thumb hole along the *red line*. **b** The migration of the axis point shown on the *left* produces the track flare pattern shown on the *right* as the ball continues down the lane

would remain fixed and the ball would contact the lane along a single circular arc on the surface of the ball. This however is not the case in general as illustrated in Fig. 6b which shows the computed locus of points on the surface of the ball that contact the lane. This so-called "ball track" or "track flare pattern" is frequently observed by bowlers by carefully inspecting the pattern of oil distributed on an initially clean (or sanded) ball surface. Track flare is desirable since it brings dry (oil-free) ball surface in contact with the lane thereby increasing the friction that causes the ball to hook.

4 Analysis of hook potential

As emphasized above, the potential of a ball to hook (and thus to strike in the "pocket") is strongly influenced by the release conditions $(\vec{\omega}, \vec{v})$. Here, we establish an explicit relationship between a measure of "hook potential" and the release conditions by analyzing the initial friction force acting on the ball. Moreover, we demonstrate that this measure of hook potential can be computed using measurements from the embedded IMU and we illustrate this capability with an example.

In reference to Fig. 7, a friction force $\vec{F}_{\mathrm{f}}$ acts on the ball at the ball-lane contact point P and it is directed opposite to the velocity $\vec{v}_{\mathrm{p}}$ of the ball at this contact point. Let C denote the ball center and let the dashed curve denote the path of the ball center projected onto the lane. The unit vectors $\hat{e}_{\mathrm{t}}$ and $\hat{e}_{\mathrm{n}}$, which lie in the plane of the lane, point along the tangent and normal to the ball center path, respectively. Thus, the velocity of the ball center can be written as

$$\vec{v} = v\hat{e}_{\mathrm{t}}, \tag{1}$$

whereas the velocity of the contact point can be written as

$$\vec{v}_{\mathrm{p}} = v_{\mathrm{p}}(\cos\alpha\hat{e}_{\mathrm{t}} - \sin\alpha\hat{e}_{\mathrm{n}}) \tag{2}$$

where α is the angle between $\vec{v}$ and $\vec{v}_{\mathrm{p}}$. The friction force is directed exactly opposite to $\vec{v}_{\mathrm{p}}$, therefore

$$\vec{F}_{\mathrm{f}} = \mu mg(-\cos\alpha\hat{e}_{\mathrm{t}} + \sin\alpha\hat{e}_{\mathrm{n}}) \tag{3}$$

where μ denotes the coefficient of kinetic friction.[1] It is the component of the friction force normal to the path namely $\mu mg\sin\alpha$, that causes the ball to hook. In contrast, the component of the friction force tangent to the path; namely $-\mu mg\cos\alpha$, causes the ball to decelerate (slightly).

Equation 3 shows that the hook potential of a bowling ball is fundamentally related to the angle α which is the angle formed between $\vec{v}$ and $\vec{v}_{\mathrm{p}}$. These two velocities are related through

$$\vec{v}_{\mathrm{p}} = \vec{v} + \vec{\omega} \times \vec{r} \tag{4}$$

where $\vec{\omega}$ is the angular velocity of the ball and

$$\vec{r} = -r\hat{k} \tag{5}$$

is the position of P relative to C (with r being the radius of the ball and $\hat{k}$ being a unit vector pointing upwards from the lane). We shall evaluate Eq. 4 to solve for $\sin\alpha$ by first referring to Fig. 8 which illustrates the orientation of $\vec{\omega}$ relative to $\vec{v}$.

The point where the angular velocity vector pierces the ball surface is the axis point described above and it is again labeled A in this figure. The point where the ball center velocity pierces the ball surface is now termed the "velocity point" and it is labeled V in the figure. A third

[1] In arriving at (3), we assume that the magnitude of the normal force remains mg. Thus, we ignore any dynamic variations of the normal force that may develop due to the possible offset of the mass center from the geometric center of the ball. This approximation is well justified. The offset is often <1 mm [5, 6] and, for a ball with a large rev rate of 300 RPM (31.4 rad/s), this leads to a centripetal acceleration component for the mass center of a 0.99 m/s^2. Hence, in this case, the variation in the normal force would be 10% or less of the weight of the ball.

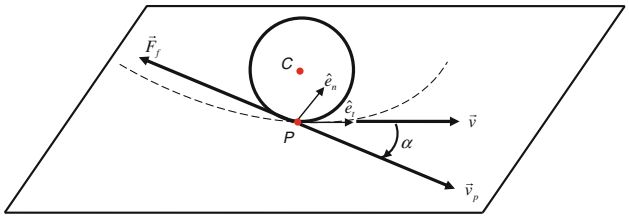

Fig. 7 Ball on lane showing relative orientation of velocity of the ball center $\vec{v}$ (projected onto plane of the lane), velocity of the contact point $\vec{v}_{\mathrm{p}}$, and the friction force $\vec{F}_{\mathrm{f}}$. These vector quantities lie in the plane of the lane which is coincident with the plane formed by the unit vectors $(\hat{e}_{\mathrm{t}}, \hat{e}_{\mathrm{n}})$ that are tangent and normal to the ball center path (*dashed curve*)

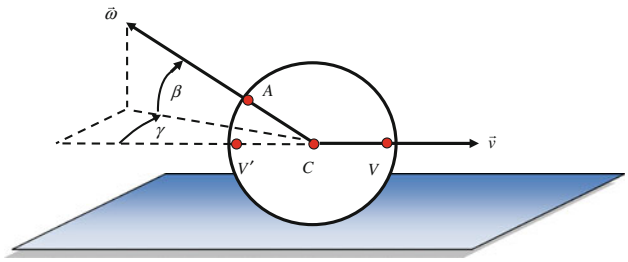

Fig. 8 Side view of ball on lane showing the ball center velocity $\vec{v}$ and the angular velocity $\vec{\omega}$. $\vec{v}$ pierces the ball at the velocity point V and $\vec{\omega}$ pierces the ball at the axis point A. The point V' is diametrically opposite V. The axis rotation γ and the axis tilt β are spherical coordinates that locate A relative to V'

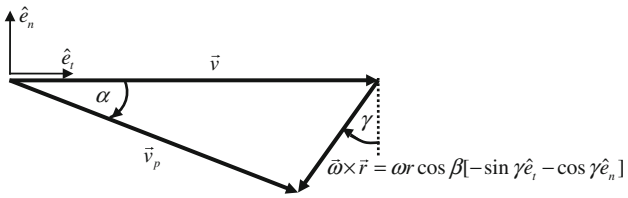

Fig. 9 Triangle representing the vector sum $\vec{v}_{\mathrm{p}} = \vec{v} + \vec{\omega} \times \vec{r}$. The angle α denotes the angle formed between $\vec{v}$ and $\vec{v}_{\mathrm{p}}$ as defined in Fig. 7, and γ and β are the axis rotation and tilt, respectively, as defined in Fig. 8

point, labeled V', is located diametrically opposite V. For a right-handed bowler, we introduce the "axis tilt" β and the "axis rotation" γ as two spherical coordinates that locate A relative to V'. [2]The axis tilt β is the elevation angle which lies in a vertical plane, whereas the rotation angle γ is the azimuthal angle which lies in the horizontal plane. In the bowling industry, there appears to be multiple definitions for "axis rotation", but the definition for axis tilt is unique and agrees with that illustrated in Fig. 8. Using these definitions for axis tilt and axis rotation, one can show that the second term in Eq. 4 can be expanded as

$$\vec{\omega} \times \vec{r} = \omega r \cos\beta[-\sin\gamma\hat{e}_t - \cos\gamma\hat{e}_{\mathrm{n}}] \tag{6}$$

Equation 4 represents the simple vector sum for $\vec{v}_p$ shown graphically in Fig. 9. Employing the law of sines for the triangle illustrated in Fig. 9, one can show that

$$\sin\alpha = \frac{\omega r \cos\beta\cos\gamma}{\sqrt{v^2 + 2v\omega r\cos\beta\sin\gamma + (\omega r\cos\beta)^2}} \tag{7}$$

The result, Eq. 7, demonstrates that the hook potential (i.e. $\sin\alpha$) depends on the ball release conditions as manifested by the rev rate ω, the axis tilt β, the axis rotation γ, and the ball center speed v. These quantities are readily determined using the inertial sensor data from the embedded IMU. In particular, the angular rate gyros provide the magnitude (ω) and the direction (β, γ) of the angular velocity relative to the computed direction of the ball center velocity $(\vec{v})$.

Next, we compute the maximum hook potential by simply maximizing $\sin\alpha$. For a given rev rate ω and ball center speed v, the maximum hook potential is achieved when $\beta = 0$ and when

$$\sin(\alpha_{\mathrm{optimum}}) = \sin(\gamma_{\mathrm{optimum}}) = \frac{\omega r}{v} \tag{8}$$

This simple result leads to two important conclusions. First, any axis tilt decreases the hook potential of the ball. This follows immediately from Eq. 7 or from Fig. 9, which both show that the leg of the triangle opposite α is maximized when axis tilt is eliminated ($\beta = 0$). This is also obvious from Eq. 6, which shows that the added speed due to rotation is maximized when axis tilt is eliminated. Second, there exists an optimum axis rotation $\gamma_{\mathrm{optimum}}$ that further maximizes the hook potential when axis tilt is eliminated. The optimum axis rotation is

$$\gamma_{\mathrm{optimum}} = \arcsin\left(\frac{\omega r}{v}\right), \tag{9}$$

which also equals $\alpha_{\mathrm{optimum}}$. As a result, the maximum initial sideways friction force that a bowler can generate is given by

$$F_{\mathrm{max\,sideways}} = \mu mg\sin\alpha_{\mathrm{optimum}} = \mu mg\frac{\omega r}{v} \tag{10}$$

4.1 Example

Consider again the throw by the professional bowler previously illustrated in Figs. 5 and 6. Once the ball center velocity has been computed (Fig. 5), one can immediately establish the velocity point V as well as its image point V'. Then, using Eq. 9, one can locate the optimum location of the bowler's axis point which is located at the center of the

[2] Note that, for a left-hander, it will be more convenient to introduce the same angles but relative to V instead of V' since A will now be approximately diametrically opposite to the position shown in Fig. 8.

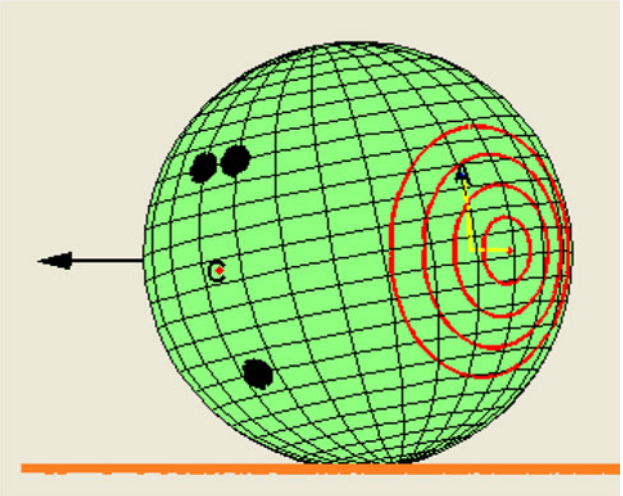

Fig. 10 Image shows the optimum (center of bullseye) versus the actual (A) axis point for the example throw by a professional bowler previously illustrated in Figs. 5 and 6

bullseye illustrated in Fig. 10. The actual location of the bowler's axis point in this example, again denoted by A, is reasonably close to the optimum location. In particular, it lies 22° above (i.e. has 22° of axis tilt) and 13° to the left of the optimum as illustrated by the yellow line segments.

The capability to precisely measure the location of the bowler's axis point relative to its optimum location provides a powerful means to assess bowler skill. Moreover, high-level bowlers intentionally vary their release to increase or decrease ball hook depending on the prevailing oil conditions in the lane. Inspection of the hook potential, such as illustrated in Fig. 10, enables a bowler to quickly deduce how the axis point must now change (i.e. how to change the ball release) to achieve a desirable result.

5 Summary and conclusions

This paper describes an exciting new technology for measuring the dynamics of a bowling ball. The technology, a highly miniaturized and wireless IMU embedded in a bowling ball, transmits both acceleration and angular velocity data that define the dynamics of the ball, including the bowler's delivery and the motion of the ball down the lane.

The analysis of the bowler's throw reveals the enormous angular velocity developed by professional bowlers during the "lift" just prior to ball release. The magnitude of the angular velocity, the so-called "rev rate," and the direction of this vector, defining the so-called "bowler's axis point," are directly measured by the IMUs angular rate gyros. The velocity of the ball center is a computed result that employs both measured acceleration and angular velocity data. Together, the angular velocity and ball center velocity $(\vec{\omega}, \vec{v})$ at ball release define the initial conditions that determine the motion of the ball in the lane thereafter (together with all factors influencing lane friction). Professional bowlers develop considerable "hook" in the ball path via the component of friction normal to this path. An analytical definition of the "hook potential" is derived which can also be directly measured using data from the IMU. Moreover, this analysis reveals that the optimum location for the bowler's axis point (to maximize ball hook) is a function of the rev rate (ω) and ball speed (v) at release. In particular, the hook is maximized by eliminating axis tilt ($\beta = 0$) and aligning the axis rotation with the optimum value $\gamma_{\text{optimum}} = \arcsin(\omega r/v)$. Example results from a professional bowler also reveal how the axis point (i.e. the spin axis) migrates as the ball moves down the lane resulting in a computed track flare pattern on the surface of the ball. Knowledge of the track flare from these measurements may also aid ball design. In summary, this new technology provides a new means to assess both bowler performance and ball performance by precisely measuring the ball dynamics.

Finally, the sensor presented herein (19 × 24 mm and 4.5 g including battery) is believed to be the world's smallest, wireless IMU. This highly miniaturized and wireless design enables parallel sports training systems for many sports, including basketball, baseball, crew, cricket, golf, fly fishing, soccer, softball, tennis, rowing, among others.

Acknowledgments The authors wish to acknowledge the research support provided by Ebonite International and the earlier contributions of Mr. Darren Goldenberg to our project.

Conflict of interest The authors declare that they have no conflict of interest.

References

1. (2010) reported statistics courtesy of the United State Bowling Congress, http://www.bowl.com/about/index.jsp#. Accessed 10 January 2010
2. Synge JL, Griffith BA (1949) Principles of mechanics. McGraw-Hill, New York, pp 447–450
3. Kane TR (1961) Analytical elements of mechanics, vol 2. Academic Press, New York, pp 211–216
4. Hopkins DC, Patterson JD (1977) Bowling frames: paths of a bowling ball. Am J Phys 45(3):263–266
5. Huston RL, Passerello C, Winget JM, Sears J (1979) On the dynamics of a weighted bowling ball. ASME J Appl Mech 46:937–943
6. Frohlich C (2004) What makes bowling balls hook? Am J Phys 72(9):1171–1177
7. Zecchini E, Foutch GL (1991) The bowling ball's path. Chemtech 21:731–735

8. Walker J (1988) Why sidespin helps the bowler—and how to keep scoring strikes. Sci Am Amateur Sci 258:110–113
9. Cross R (1998) The trajectory of a ball in lawn bowls. Am J Phys 66(8):735–738
10. Brearley MN, Bolt BA (1958) The dynamics of a bowl. Q J Mech Appl Math 11:351–363
11. Brearley MN (1961) The motion of a biased bowl with perturbing projection conditions. Proc Cambridge Philos Soc 57:131–151
12. Chu DPK, Zhang B-M, Mau K (2002) Tenpin bowling technique on elite players. In: Proceedings of 2002 international conference on biomechanics in sports, pp 123–125
13. Fuss FK (2009) Design of an instrumented bowling ball and its application to performance analysis in tenpin bowling. Sports Technol. doi:10.1002/jst.104
14. Song C (1997) Commercial vision of silicon based inertial sensors. Tech Dig 9th Intl Conf Solid State Sensors and Actuators 2:839–842
15. Yazdi N, Ayazi F, Najafi K (1998) Micromachined inertial sensors. Proc IEEE 86(8):1640–1659
16. Barbour N, Schmidt G (2001) Inertial sensor technology trends. IEEE Sens J 1(4):332–339
17. Savage PG (2002) Strapdown analytics. Strapdown Associates Inc, Maple Plane
18. Rogers RM (2003) Applied mathematics in integration navigation systems. American Institute of Aeronautics and Astronautics, Reston, VA
19. Titterton DH, Weston JL (2004) Strapdown inertial navigation technology, 2nd edn. The Institution of Electrical Engineers, Stevenage UK and The American Institute of Aeronautics and Astronautics, Reston, VA
20. Perkins NC (2006) Electronic measurement of the motion of a moving body of sports equipment. US patent no. 7,021,140
21. Perkins NC (2007) Electronic measurement of the motion of a moving body of sports equipment. US patent no. 7,234,351
22. King KW (2008) The design and application of wireless MEMS inertial measurement units for the measurement and analysis of golf swings. Dissertation, University of Michigan
23. King KW, Yoon SW, Perkins NC, Najafi K (2008) Wireless MEMS inertial sensor system for golf swing dynamics. Sens Actuators A Phys 141:619–630
24. King KW, Perkins NC (2008) Putting stroke analysis using wireless MEMS inertia sensor systems. In: Proceedings of the world scientific congress on golf V, Phoenix, AZ, USA, pp 270–278
25. King KW, Yoon SW, Perkins NC, Najafi K (2004) The dynamics of the golf swing as measured by strapdown inertial sensors. In: Proceedings of the fifth international conference on the engineering of sport, vol 2. Davis, CA, USA, pp 276–282
26. Perkins NC, Richards B (2003) Dissecting the casting stroke: electronic measurements provide new insights. Fly Fisherman Magazine, December 2003:34–37, 66
27. Anderson D, Perkins NC, Richards B (2006) Quantitative understanding of the fly casting stroke through measurements and robotic casting. J Sports Eng 9(2):97–106
28. Ohgi Y, Ichikawa H, Miyaji (2002) Microcomputer-based acceleration sensor device for swimming stroke monitoring. JSME Int J Ser C 45:960–966
29. Meamarbashi A (2009) A novel inertial technique to measure very high linear and rotational movements in sports, part I: the hardware. J Appl Sci 9(9):1741–1746
30. Hon TM, Senanyake ASMN, Flyger N (2009) Biomechanical analysis of 10-pin bowling using wireless inertial sensor. In: Proceedings of the 2009 IEEE/ASME international conference on advanced intelligent mechatronics, Singapore, pp 1130–1135